

Synthesis and characterization of
mist chemical vapor deposited
aluminum titanium oxide films

journal or publication title	Japanese Journal of Applied Physics
volume	58
number	7
page range	70905
year	2019-06-28
URL	http://hdl.handle.net/2298/00043655

doi: 10.7567/1347-4065/ab29e3

Synthesis and characterization of mist chemical vapor deposited aluminum titanium oxide films

Zenji Yatabe ^{1*†}, Koshi Nishiyama ^{2†}, Takaaki Tsuda ², Kazuki Nishimura ², and Yusui Nakamura ^{2,3}

¹ *Priority Organization for Innovation and Excellence, Kumamoto University, Kumamoto 860-8555, Japan*

² *Graduate School of Science and Technology, Kumamoto University, Kumamoto 860-8555, Japan*

³ *Kumamoto Phoenixes, Kumamoto 862-0901, Japan*

Aluminium titanium oxide ($\text{Al}_{1-x}\text{Ti}_x\text{O}_y$, an alloy of Al_2O_3 and TiO_2), an attractive high- κ dielectric material, were synthesized by mist chemical vapor deposition, utilizing Al_2O_3 and TiO_2 precursors. X-ray diffraction investigations revealed that the $\text{Al}_{1-x}\text{Ti}_x\text{O}_y$ ($0 < x < 0.72$) films deposited at 400 °C has amorphous-phase structure. It was found that the bandgap of the $\text{Al}_{1-x}\text{Ti}_x\text{O}_y$ films decreases with increasing Ti composition. Moreover, the obtained refractive index, mass density and bandgap of Al_2O_3 and TiO_2 films are all comparable to those reported for high-quality Al_2O_3 and TiO_2 films deposited by atomic layer deposition.

*E-mail: yatabe@cs.kumamoto-u.ac.jp

†These authors contributed equally to this work.

For realizing high-performance metal–oxide–semiconductor field–effect transistors (MOSFETs), one of the main challenges is finding a gate dielectric material possessing both high permittivity (κ) and wide bandgap (E_G). However, there is a well-known trade-off between these two properties [1]. High- κ insulators are desirable for fabrication of MOSFETs with high transconductance. On the other hand, wide bandgap and large band offset that goes with, are necessary for sufficient suppression of the gate leakage current even at forward bias [2]. One effective solution for balancing between κ and E_G is employing aluminum titanium oxide $[(\text{Al}_2\text{O}_3)_{1-x}(\text{TiO}_2)_x]$ with intermediate properties of Al_2O_3 ($\kappa \sim 9$, $E_G \sim 7$ eV) and TiO_2 ($\kappa \sim 50$, $E_G \sim 3$ eV). As a matter of fact, high-quality $\text{Al}_{1-x}\text{Ti}_x\text{O}_y$ gate insulator deposited by atomic layer deposition (ALD) method and other vacuum deposition techniques has been used for Si-based [3-5], GaAs-based [6,7] and GaN-based devices [8,9]. One alternative approach to obtain $\text{Al}_{1-x}\text{Ti}_x\text{O}_y$ thin films is the mist chemical vapor deposition (mist-CVD) technique, which can deposit various metal oxide thin films from relative non-toxic and nonpyrophoric aqueous solution under atmospheric pressure. As such, mist-CVD is regarded as relatively simple, safe and cost-effective [10-18]. Recent years have witnessed mist-CVD delivering their promise of high-quality metal oxide thin films and demonstrating their capability as an able replacement for vacuum deposition techniques. For Al_2O_3 thin films deposited by mist-CVD, Kawaharamura et al. [10] reported AlO_x thin films having smooth surface grown on 100 mm^φ substrates. Furthermore, Oh et al. [11] and Kim et al. [12] reported AlO_x thin films having breakdown field of approximately 9 MV/cm synthesized by mist-CVD. For TiO_2 thin films deposited by mist-CVD, several groups [13-15] have reported both amorphous and crystalline-phase structure TiO_2 films deposited by the mist-CVD. Liu et al. [14] successfully fabricated mist-CVD of TiO_2 -based ultraviolet photodetectors.

In this work, we report on the deposition of $\text{Al}_{1-x}\text{Ti}_x\text{O}_y$ alloy films by mist-CVD

method, utilizing Al_2O_3 and TiO_2 precursors and subsequent investigation of the chemical properties, crystallinity, mass density, refractive index and bandgap of the deposited films. We confirmed that the obtained refractive index, mass density and bandgap of Al_2O_3 and TiO_2 films are all comparable to those reported for high-quality Al_2O_3 and TiO_2 films deposited by ALD, thereby demonstrating the efficacy of using mist-CVD in synthesizing films having almost the same properties as those prepared by the more mature ALD.

In this study, $\text{Al}_{1-x}\text{Ti}_x\text{O}_y$ alloy films were prepared using a homemade fine-channel-type mist-CVD system. The homemade mist-CVD system was described in detail elsewhere [16,17]. Aluminum acetylacetonate [$\text{Al}(\text{C}_5\text{H}_7\text{O}_2)_3$, $\text{Al}(\text{acac})_3$] and titanium isopropoxide [$\text{Ti}(\text{C}_3\text{H}_7\text{O})_4$, TTIP] were used as the Al and Ti precursors, respectively. These Al and Ti precursors were dissolved in a mixture of methanol (CH_4O) with acetylacetone ($\text{C}_5\text{H}_8\text{O}_2$, acac) at TTIP : acac molar ratio of 1 : 1. The addition of acac is effective for avoiding the hydrolysis reaction of TTIP [19]. The Al precursor molar concentration in the solution was constant at 0.06 mol/L and the Ti precursor concentrations were in the range of 0.00–0.09 mol/L. The $\text{Al}_{1-x}\text{Ti}_x\text{O}_y$ films were deposited on boron-doped crystalline silicon (Si) 2-in.-diameter substrates at 400 °C with nitrogen carrier gas at a flow rate of 3 L/min. The film thicknesses were measured from a probe-type step profiler. Note that all the characterizations were performed on as-deposited samples without undergoing any post-deposition annealing process.

We initially characterized the chemical properties of mist-CVD of $\text{Al}_{1-x}\text{Ti}_x\text{O}_y$ films with a nominal thickness of 1 μm by X-ray fluorescence (XRF) equipped with a Rh anode tube (50 kV and 60 mA) and a single crystal spectrometer (Rigaku ZSX Primus II). **Figure 1** shows the dependence of Ti composition x in the mist- $\text{Al}_{1-x}\text{Ti}_x\text{O}_y$, which was determined by the quantitative XRF analysis using Al and Ti $K\alpha$ lines, on the Ti concentration ratio in the source solution, $\gamma = \text{Ti}/(\text{Al} + \text{Ti})$. The Ti composition x in the film monotonically increases as Ti

concentration ratio in the solution γ . This indicates that the Ti concentration ratio in the film can be controlled by the concentration ratio of Al and Ti precursors in the solution prepared. In almost similar fashion, Nishinaka et al. [20] also successfully controlled Mg composition in mist-CVD of $Zn_{1-x}Mg_xO$ film by changing Mg concentration ratio in a source solution.

Figure 2(a) shows the XRF Al $K\alpha$ spectra of mist- $Al_{1-x}Ti_xO_y$ films with various Ti compositions x , which was compared with that of the reference 2-mm-thick Al metal. The XRF Al $K\alpha$ spectra of the mist-CVD of $Al_{1-x}Ti_xO_y$ films are shifted by 0.38 eV toward the higher energy direction relative to that of the Al metal. The chemical shift of XRF lines is usually interpreted by the effective charges of the X-ray emitting atom [21,22]. The obtained chemical shift value of 0.38 eV are in good agreement with the reported values 0.37–0.39 eV in going from the Al metal to the Al_2O_3 [23,24], suggesting presence of Al-O bond. **Figure 2(b)** shows the Ti $K\beta$ and $K\eta$ XRF satellite spectra of mist-CVD of $Al_{1-x}Ti_xO_y$ films with various Ti compositions x , which was compared with that of the reference 2-mm-thick Ti metal. The obtained $K\eta$ satellite peak intensities are approximately 1.4 % of that of the main $K\beta$ lines for both mist- $Al_{1-x}Ti_xO_y$ and Ti-metal, which is close to the values reported for the oxide compounds of Ti and metallic Ti [25]. Although the $K\beta$ intensity is a very strong line whereas the $K\eta$ satellite intensity is a very weak for Ti atom, Kawai et al. [25] found that the $K\eta$ satellite peak depends on the neighboring Ti atom in compounds due to the radiative Auger effect. The dip between $K\beta$ and $K\eta$ of the obtained- $Al_{1-x}Ti_xO_y$ films is deeper than that of reference Ti metal, suggesting the presence of Ti-O bond in the obtained films. Kawai et al. [25] also reported a reasonably similar deeper dip between $K\beta$ and $K\eta$ lines for TiO_2 . These qualitative chemical state analyses of Al and Ti atoms suggest that both Al and Ti atoms were oxidized and $Al_{1-x}Ti_xO_y$ films were formed by mist-CVD.

Next, we characterized the crystallographic properties of as-deposited mist-CVD of

$\text{Al}_{1-x}\text{Ti}_x\text{O}_y$ films with a nominal thickness of 1 μm grown on Si substrate with various Ti composition x by X-ray diffraction (XRD) equipment (Rigaku Ultima IV). **Figure 3** shows the XRD θ - 2θ scan profiles of the mist-CVD of $\text{Al}_{1-x}\text{Ti}_x\text{O}_y$ films. From the results, it is found that anatase (101)-oriented anatase TiO_2 film are deposited for $x = 1$. Zhang et al. [15] also reported predominant (101)-oriented anatase phase TiO_2 films on quartz glass substrate deposited at 300–400 $^\circ\text{C}$ by mist-CVD using TTIP-based precursor solution. On the other hand, no apparent peaks such as metallic and/or oxides of Al and Ti are present apart from that of Si for $x = 0$ to 0.72, which indicate that mist-CVD of $\text{Al}_{1-x}\text{Ti}_x\text{O}_y$ films deposited at 400 $^\circ\text{C}$ has amorphous-phase structure. This is because the deposition temperature (400 $^\circ\text{C}$) was too low for the crystallization of Al_2O_3 film reported to be ~ 800 $^\circ\text{C}$ [26,27], though it was still higher than the reported temperature for anatase TiO_2 film (~ 300 – 350 $^\circ\text{C}$) [14,15]. Indeed, Shi et al. [4] successfully obtained crystalline $\text{Al}_{1-x}\text{Ti}_x\text{O}_y$ film on Si substrate via pulsed laser deposition and the subsequent post-deposition annealing at 900 $^\circ\text{C}$. However, the amorphous-phase structure is a highly feasible and desirable for the application of $\text{Al}_{1-x}\text{Ti}_x\text{O}_y$ as a gate dielectric in MOSFETs. Hori et al. [26] pointed out that microcrystallized Al_2O_3 film causes a marked increase in the leakage current of the $\text{Al}_2\text{O}_3/\text{GaN}$ MOS structure, which can be problematic especially at high voltage applications. The grain boundaries in the microcrystallized Al_2O_3 layer can serve as high-leakage paths and can lead to premature device breakdown.

Since carbon impurities [11,28] in the films and film porosity [12] may affect the refractive index, ellipsometry and X-ray reflectivity (XRR) measurements were performed. Ellipsometry measurements were carried out using a spectroscopic ellipsometer (ULVAC UNECS-1500M) with wavelength ranges from 530 to 750 nm. The mass densities were obtained by XRR equipment (Rigaku SmartLab) at an angle of incidence of 0° – 4° . The refractive index and mass density of 40 nm thick $\text{Al}_{1-x}\text{Ti}_x\text{O}_y$ films on the Si substrate as a

function of Ti composition x in the film are shown in **Figs. 4(a)** and **4(b)**, respectively. Note that index values at 633 nm were plotted for comparing reported values. As expected, the refractive index and mass density of the obtained films increases with the rise of Ti composition x . Note that the obtained refractive index and mass density of Al_2O_3 and TiO_2 films are all comparable to those reported for high-quality amorphous Al_2O_3 [26,29–31] and anatase TiO_2 [32,33] films deposited by ALD as plotted in **Figs. 4(a)** and **4(b)**. It is likely that the obtained mist-CVD of $\text{Al}_{1-x}\text{Ti}_x\text{O}_y$ films are relatively dense as well as having low carbon impurity contamination. Even though further investigations are still needed to clarify detailed relationships between the refractive index and mass density of obtained films, Gladstone–Dale and Lorentz–Lorenz model may qualitatively explain relationship between density and refractive index [28,29]. Because these models indicate that refractive index linearly depends on the film density.

Pu et al. [34] and Peng et al. [35] obtained the direct optical bandgap of spin coated- $\text{Al}_{1-x}\text{Ti}_x\text{O}_y$ films from transmittance spectra with simple Tauc plots [36]. We also determined the direct optical bandgap of mist- $\text{Al}_{1-x}\text{Ti}_x\text{O}_y$ films for $x = 0.19$ to 0.72 with nominal thickness of $1\ \mu\text{m}$ on sapphire substrate using ultraviolet/visible spectrophotometer equipment (Shimadzu UV-3600) with wavelength ranges from 185 to 2500 nm. Note that anatase TiO_2 ($x = 1$) film was detected as shown **Fig. 3**. Anatase TiO_2 is an indirect bandgap material. We thus calculate indirect optical bandgap for anatase TiO_2 ($x = 1$) film on sapphire substrate. In addition, the bandgap of obtained mist- Al_2O_3 ($x = 0$) film is more than 6 eV, rendering Tauc's formula unsuitable in this situation. Accordingly, the bandgap of the mist-CVD Al_2O_3 ($x = 1$) with a nominal thickness of 38 nm was estimated from the energy-loss peak in the O 1s XPS spectrum. Details of the XPS measurements are provided in Ref. 18. We then compared our present results with those reported in literature from ALD of amorphous Al_2O_3 , [26,29,30] anatase TiO_2 [32]

and spin coated amorphous $\text{Al}_{1-x}\text{Ti}_x\text{O}_y$ [34] films as plotted in **Fig. 5**. Our results showed that bandgap of the $\text{Al}_{1-x}\text{Ti}_x\text{O}_y$ films decreased with increasing Ti composition x , which was similar to the behavior of the bandgap of spin coated amorphous $\text{Al}_{1-x}\text{Ti}_x\text{O}_y$ films. Although further investigation is necessary to characterize electrical properties of the obtained films, the obtained refractive index, mass density and bandgap of amorphous Al_2O_3 ($x = 0$) and TiO_2 ($x = 1$) films are comparable to those reported for high-quality amorphous Al_2O_3 and anatase TiO_2 films deposited by ALD. This significant fact indicates that atmospheric pressure solution-processed mist-CVD technique is promising for depositing high-quality $\text{Al}_{1-x}\text{Ti}_x\text{O}_y$ gate insulator and surface passivation layer. As future work, we will carry on electrical properties characterization of the mist CVD prepared $\text{Al}_{1-x}\text{Ti}_x\text{O}_y$ films.

In summary, aluminium titanium oxide ($\text{Al}_{1-x}\text{Ti}_x\text{O}_y$, an alloy of Al_2O_3 and TiO_2) films as a candidate for high- κ dielectric were synthesized by mist-CVD, utilizing Al_2O_3 and TiO_2 precursors. XRD studies revealed that the $\text{Al}_{1-x}\text{Ti}_x\text{O}_y$ ($0 < x < 0.72$) films deposited at 400 °C has amorphous-phase structure. It was found that the bandgap of the $\text{Al}_{1-x}\text{Ti}_x\text{O}_y$, films decreases with increasing Ti composition. The obtained refractive index, mass density and bandgap of Al_2O_3 and TiO_2 films are all comparable to those reported for high-quality Al_2O_3 and TiO_2 films deposited by ALD, suggesting the viability of mist-CVD in synthesizing $\text{Al}_{1-x}\text{Ti}_x\text{O}_y$ with properties that could match those prepared by their more conventional but costly counterparts.

Acknowledgements

One of the authors (ZY) sincerely thank Professors Tamotsu Hashizume and Masamichi Akazawa of the Research Center for Integrated Quantum Electronics (RCIQE), Hokkaido University and Professor Joel T. Asubar of the Graduate School of Engineering, University of Fukui for their valuable support. This work was supported by JSPS KAKENHI Grant Number

JP19K04473.

References

- [1] J. Robertson, Rep. Prog. Phys. 69, 327 (2006).
- [2] T. Hashizume, S. Ootomo, T. Inagaki, and H. Hasegawa, J. Vac. Sci. Technol. B 21 1828 (2003).
- [3] O. Auciello, W. Fan, B. Kabius, S. Saha, J. A. Carlisle, R. P. H. Chang, C. Lopez, E. A. Irene, and R. A. Baragiola, Appl. Phys. Lett. 86, 042904 (2005).
- [4] L. Shi, Y. D. Xia, B. Xu, J. Yin, and Z. G. Liu, J. Appl. Phys. 101, 034102 (2007).
- [5] I. Jōgi, K. Kukli, M. Kemell, M. Ritala, and M. Leskelä, J. Appl. Phys. 102, 114114 (2007).
- [6] C. Mahata, S. Mallik, T. Das, C. K. Maiti, G. K. Dalapati, C. C. Tan, C. K. Chia, H. Gao, M. K. Kumar, S. Y. Chiam, H. R. Tan, H. L. Seng, D. Z. Chi, and E. Miranda, Appl. Phys. Lett. 100, 062905 (2012).
- [7] T. Ui, M. Kudo, and T. Suzuki, Phys. Status Solidi C 10, 1417 (2013).
- [8] S. P. Le, T. Ui, T. Q. Nguyen, H.-A. Shih, and T. Suzuki, J. Appl. Phys. 119, 204503 (2016).
- [9] S. P. Le, D. D. Nguyen, and T. Suzuki, J. Appl. Phys. 123, 034504 (2018).
- [10] T. Kawaharamura, T. Uchida, M. Sanada, and M. Furuta, AIP Adv. 3, 032135 (2013).
- [11] K.-T. Oh, H. Kim, D. Kim, J. H. Han, J. Park, J.-S. Park, Ceram. Int. **43**, 8932 (2017).
- [12] D.-H. Kim, H.-J. Jeong, J. Park, and J.-S. Park, Ceram. Int. **44**, 459 (2018).
- [13] B.-H. Kim, J.-Y. Lee, Y.-H. Choa, M. Higuchi, N. Mizutani, Mater. Sci. Eng. B-Adv. Funct. Solid-State Mater. 107, 289 (2004).
- [14] H.-Y. Liu, Y.-L. Hsu, H.-Yi Su, R.-C. Huang, F.-Y. Hou, G.-C. Tu, and W.-H. Liu, IEEE Sens. J. 18, 4022 (2018).
- [15] Q. Zhang and C. Li, Nanomaterials 8, 827 (2018).
- [16] Z. Yatabe, T. Tsuda, J. Matsushita, T. Sato, T. Otabe, K. Sue, S. Nagaoka, and Y. Nakamura, Phys. Status Solidi C **14**, 1600148 (2017).
- [17] H. Tanoue, M. Takenouchi, T. Yamashita, S. Wada, Z. Yatabe, S. Nagaoka, Y. Naka, and Y. Nakamura, Phys. Status Solidi A **214**, 1600603 (2017).
- [18] Z. Yatabe, K. Nishiyama, T. Tsuda, and Y. Nakamura, to be published in J. Ceram. Soc. Jpn.
- [19] K. Aisu, T. S. Suzuki, E. Nakamura, H. Abe, and Y. Suzuki, J. Ceram. Soc. Jpn., 121, 915 (2013).
- [20] H. Nishinaka, Y. Kamada, N. Kameyama, and S. Fujita, Phys. Status Solidi B 247, 1460 (2010).
- [21] G. Leonhardt and A. Meisel, J. Chem. Phys. **52**, 6189 (1970).

- [22] Z. Liu, S. Sugata, K. Yuge, M. Nagasono, K. Tanaka, and J. Kawai, *Phys Rev. B* **69**, 035106 (2004).
- [23] Y. Gohshi, *Spectrochim. Acta B* **36**, 763 (1981).
- [24] T. Yamamoto, H. Miyauchi, T. Yamamoto, and J. Kawai, *Adv. X-Ray. Chem. Anal. Japan* **41**, 177 (2010).
- [25] J. Kawai, T. Nakajima, T. Inoue, H. Adachi, M. Yamaguchi, K. Maeda, and S. Yabuki, *Analyst* **119**, 601 (1994).
- [26] Y. Hori, C. Mizue, and T. Hashizume, *Jpn. J. Appl. Phys.* **49**, 080201 (2010).
- [27] S. Toyoda, T. Shinohara, H. Kumigashira, M. Oshima, and Y. Kato, *Appl. Phys. Lett.* **101**, 231607 (2012).
- [28] G. He, X. Wang, M. Oshima, and Y. Shimogaki, *Jpn. J. Appl. Phys.* **49**, 031502 (2010).
- [29] S. K. Kim, S. W. Lee, C. S. Hwang, Y.-S. Min, J. Y. Won, and J. Jeong, *J. Electrochem. Soc.* **153**, F69 (2006).
- [30] J. Yang, B. S. Eller, M. Kaur, R. J. Nemanich, *J. Vac. Sci. Technol. A* **32**, 021514 (2014).
- [31] S. Kaneki, J. Ohira, S. Toiya, Z. Yatabe, J. T. Asubar, and T. Hashizume, *Appl. Phys. Lett.* **109**, 162104 (2016).
- [32] J. Aarika, A. Aidlaa, A.-A. Kiisler, T. Uustarea, and V. Sammelselg, *Thin Solid Films* **305**, 270 (1997).
- [33] B. Abendroth, T. Moebus, S. Rentrop, R. Strohmeyer, M. Vinnichenko, T. Weling, H. Stöcker, and D. C. Meyer, *Thin Solid Films* **545**, 176 (2013).
- [34] H. Pu, H. Li, Z. Yang, Q. Zhou, C. Dong, and Q. Zhang, *ECS Solid State Lett.* **2**, N35 (2013).
- [35] J. Peng, C. Sheng, J. Shi, X. Li, and J. Zhang, *J. Sol-Gel Sci. Technol.* **71**, 458 (2014).
- [36] J. Tauc, R. Grigorovici, and A. Vancu, *Phys. Status Solidi A* **15**, 627 (1966).

Figure captions

Fig. 1 Ti composition x in mist- $\text{Al}_{1-x}\text{Ti}_x\text{O}_y$ films as a function of the Ti concentration ratio in the precursor solution, $\gamma = \text{Ti}/(\text{Al} + \text{Ti})$.

Fig. 2 (a) Al $K\alpha$ XRF spectra of mist- $\text{Al}_{1-x}\text{Ti}_x\text{O}_y$ film and reference Al-metal. (b) Ti $K\beta$ and $K\eta$ XRF spectra of mist- $\text{Al}_{1-x}\text{Ti}_x\text{O}_y$ film and reference Ti-metal.

Fig. 3 XRD profiles of mist- $\text{Al}_{1-x}\text{Ti}_x\text{O}_y$ films deposited on Si substrate.

Fig. 4 (a) Refractive index of mist- $\text{Al}_{1-x}\text{Ti}_x\text{O}_y$ films as a function of the Ti composition x in the film with reported ALD value [26,29,30-32] and (b) mass density of mist- $\text{Al}_{1-x}\text{Ti}_x\text{O}_y$ films as a function of the Ti composition x in the film with reported ALD value [30,33]. The solid lines are shown as guide to the eye.

Fig. 5 Band gap of mist- $\text{Al}_{1-x}\text{Ti}_x\text{O}_y$ films as a function of the Ti composition x . Those synthesized using ALD [26,29,30] and spin-coater [34] are also shown for comparison. The solid line is shown as guide to the eye.

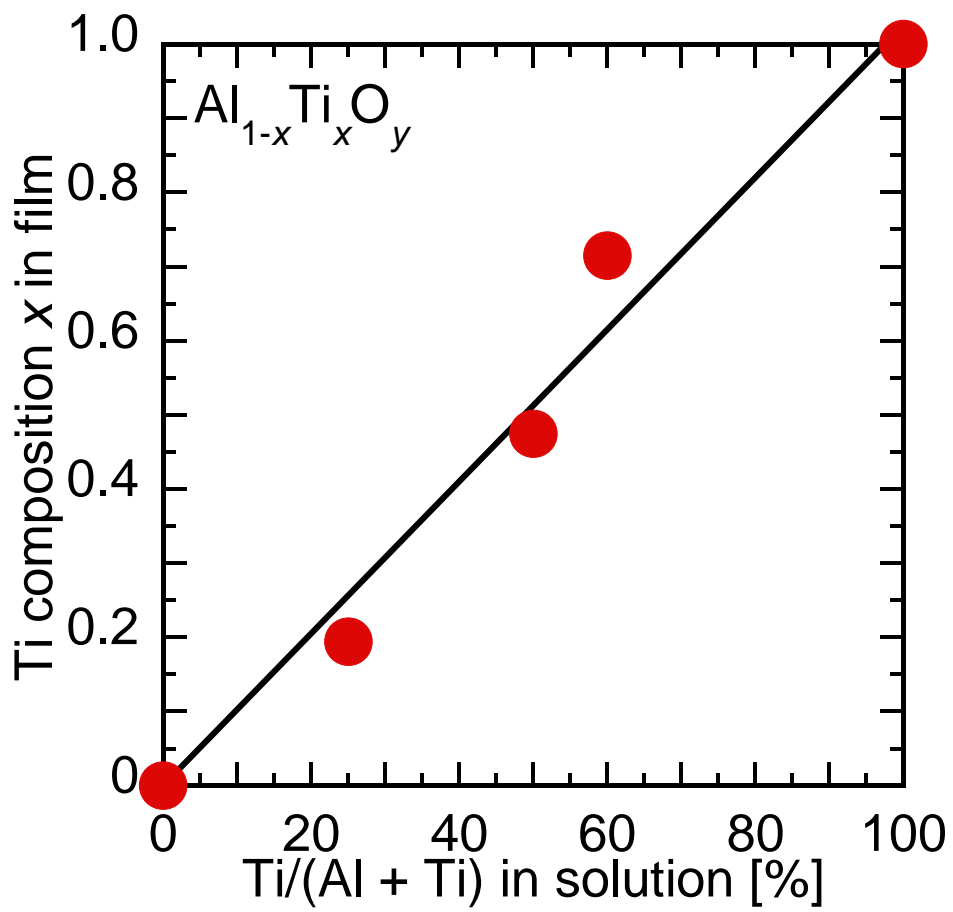


Figure 1

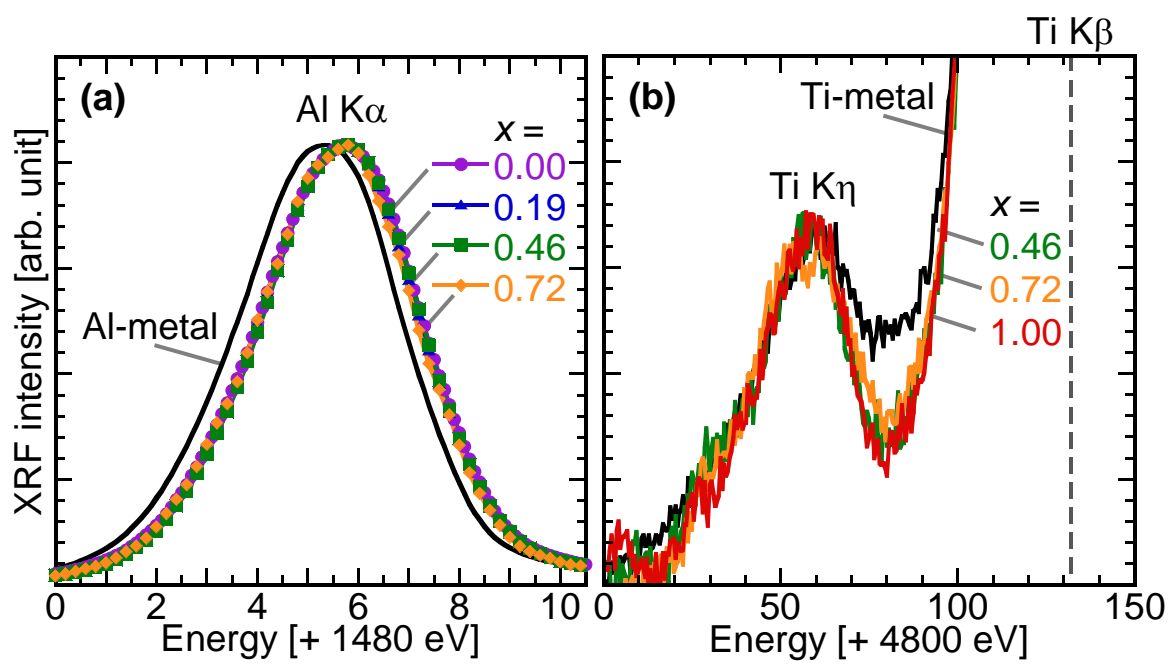


Figure 2

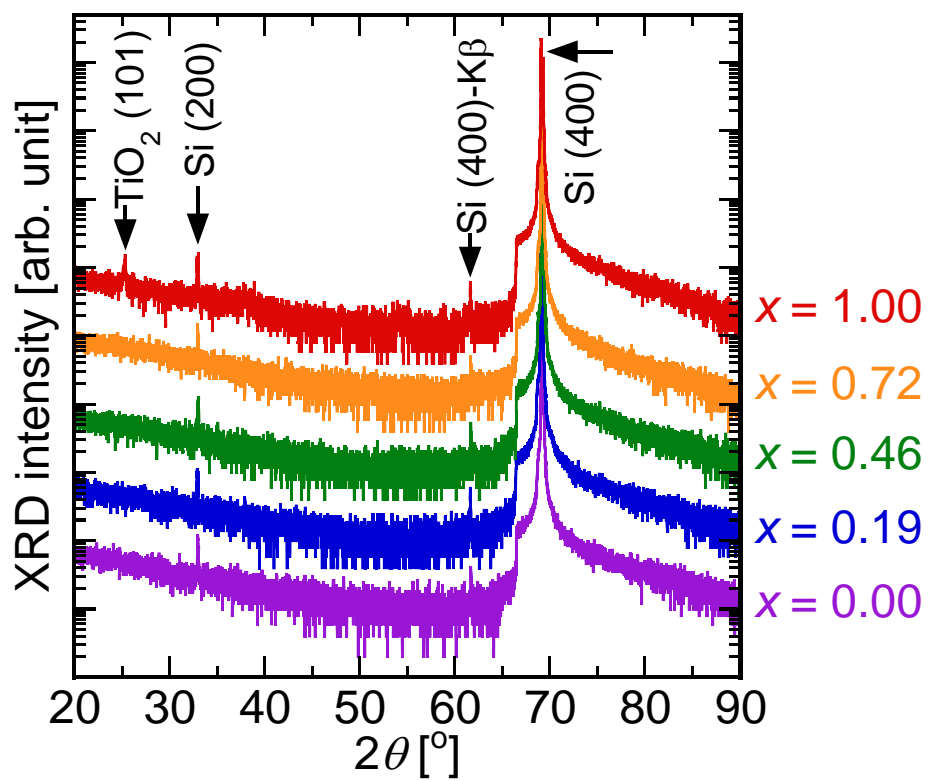


Figure 3

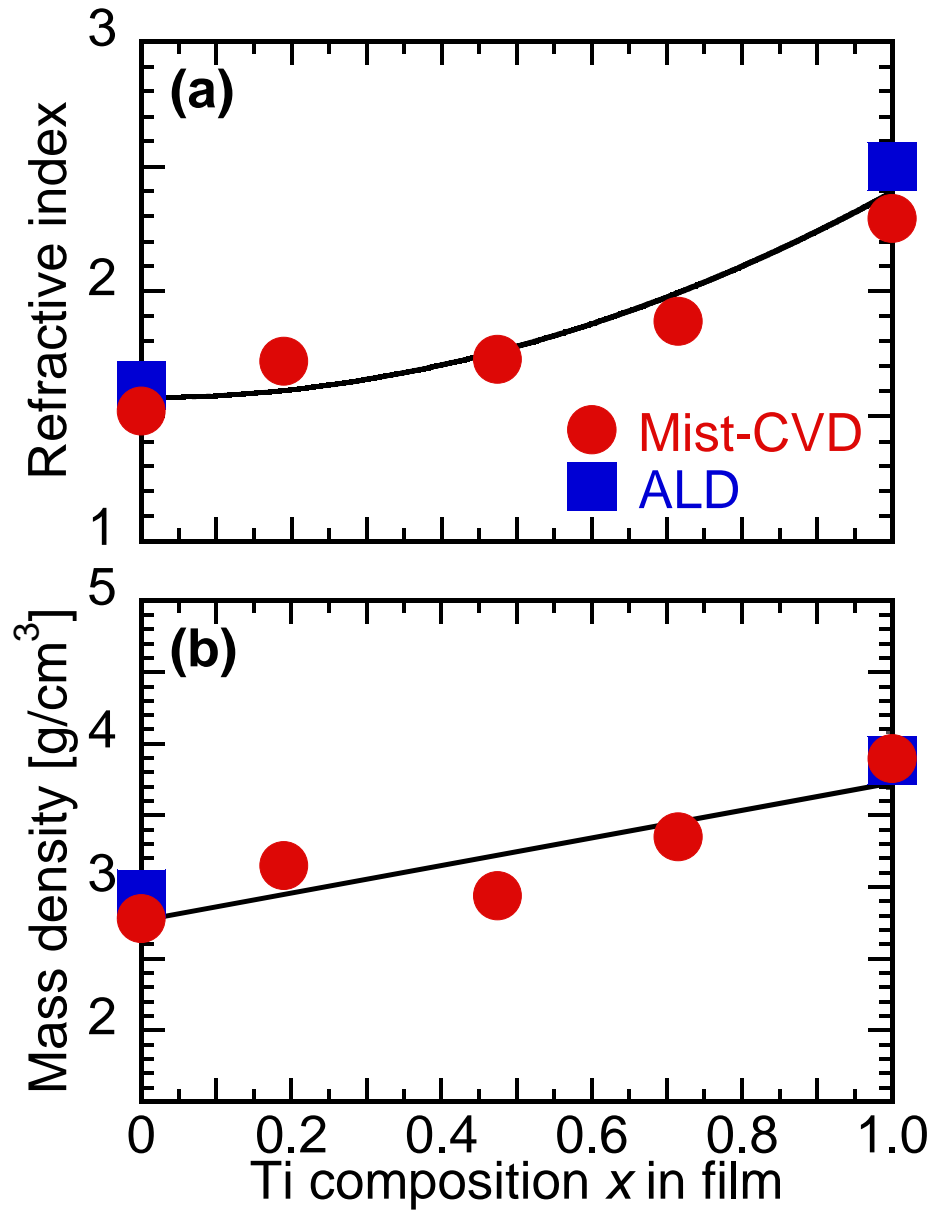


Figure4

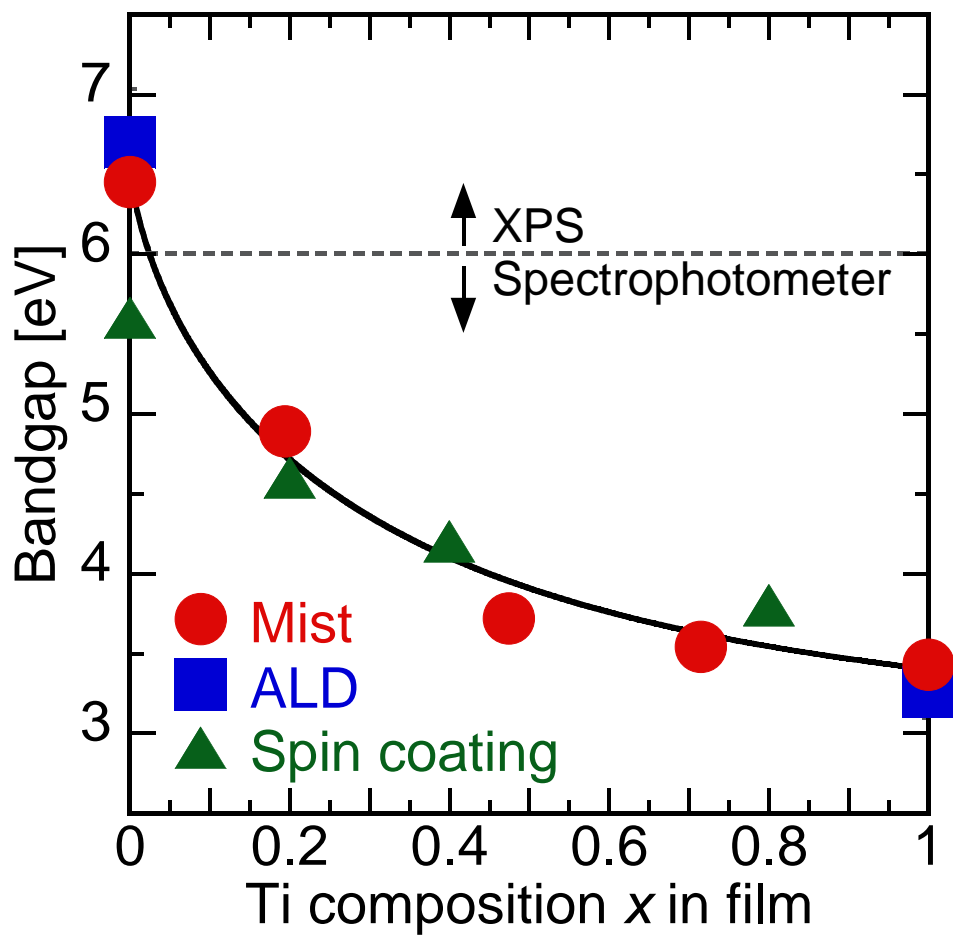


Figure 5